**Astronomy & Astrophysics**

# Orbital eccentricities of binary systems with a former AGB star

A. A. Bonačić Marinović, E. Glebbeek, and O. R. Pols

Sterrekundig Instituut Utrecht (SIU), Universiteit Utrecht, PO Box 80000, 3508 TA Utrecht, The Netherlands
e-mail: [bonacic;glebbeek;pols]@astro.uu.nl

**ABSTRACT**

*Context.* Many binary stellar systems in which the primary star is beyond the asymptotic giant branch (AGB) evolutionary phase show significant orbital eccentricities, whereas current binary interaction models predict that their orbits are circularised.
*Aims.* In the search for a mechanism to counteract the circularising effect of tidal interaction, we analyse how the orbital parameters in a system are modified under mass loss and mass exchange among its binary components.
*Methods.* We propose a model for enhanced mass loss from the AGB star due to tidal interaction with its companion, which allows a smooth transition between the wind and Roche-lobe overflow mass loss regimes. We explicitly follow its effect along the orbit on the change in eccentricity and orbital semi-major axis, as well as the effect of accretion by the companion. We calculate timescales for the variation in these orbital parameters and compare them to the tidal circularisation timescale.
*Results.* We find that in many cases, due to the enhanced mass loss of the AGB component at orbital phases closer to the periastron, the net eccentricity growth rate in one orbit is comparable to the rate of tidal circularisation. We show that with this eccentricity-enhancing mechanism it is possible to reproduce the orbital period and eccentricity of the Sirius system, which is expected to be circularised under the standard assumptions of binary interaction. We also show that this mechanism may provide an explanation for the eccentricities of most barium star systems, which are expected to be circularised due to tidal dissipation.
*Conclusions.* By proposing a tidally enhanced model of mass loss from AGB stars, we find a mechanism that efficiently works against the tidal circularisation of the orbit. This mechanism can explain the significant eccentricities observed in binary systems containing a white dwarf and a less evolved companion, which are predicted to be circularised due to their proximity, such as Sirius and systems with barium stars.

**Key words.** stars: binaries: general – stars: AGB and post-AGB – stars: individual: Sirius – stars: chemically peculiar

## 1. Introduction

Detached binary systems containing a white dwarf and a relatively unevolved companion, i.e., a main-sequence star or a (sub)giant, are a useful tool for understanding the binary evolution of systems with an asymptotic giant branch (AGB) star, given that their orbital and chemical properties do not change significantly from the moment that the primary finished its AGB evolution and became the current white dwarf. An example of such a system is Sirius, a 2.1 $M_\odot$ main sequence star with a 1.05 $M_\odot$ white dwarf companion in a 50-year orbit (e.g., van den Bos 1960; Gatewood & Gatewood 1978). In the standard picture of binary evolution with tidal interaction, this system should have circularised when the primary became an AGB star, as we show in Sect. 4.1 of this paper. However, this system has an eccentricity $e = 0.59$ and is not an exception.

A similar problem is faced when considering the barium-star systems, which are red giants with over-abundances of s-process elements (prominently barium) with white dwarf companions. The best current explanation for the enhancement of s-process elements in these stars is that they accreted mass from their companion when it was an AGB star. Due to the large size of AGB stars, these systems are expected to be circularised by tidal interaction for periods shorter than about 3500–4000 days (Pols et al. 2003). However, barium-star systems with periods as short as 600 days are observed to be significantly eccentric (Jorissen et al. 1998). The problems stated above are indications that a mechanism must exist that counteracts the circularising

effect of the tides by the time the primary star is on the AGB. Van Winckel et al. (1995) propose that enhanced mass loss at periastron could enhance the eccentricity and Soker (2000) shows that this works when the AGB star fills its Roche lobe during periastron passages. It has also been proposed that the tidal interaction between a binary system and a circumbinary disk could account for an eccentricity-enhancing mechanism (Waelkens et al. 1996; Waters et al. 1998). However, Soker (2000) argues that the masses of observed circumbinary disks are too low to counteract the circularisation.

Mass loss from stars in binary systems is commonly treated as single-star wind mass loss as long as the stars are inside their Roche lobes, while when one star fills its Roche lobe, the mass loss rate increases abruptly to the high values that correspond to Roche-lobe overflow. This approximation is fairly accurate for stars with a steep density gradient in their atmospheres, but it is not appropriate for the case of AGB stars, given their large atmospheric pressure scale height and their weakly bound envelope. The fact that AGB stars undergo dynamical pulsations further reduces density gradient in the layers above the photosphere (e.g., Bowen 1988). We propose a prescription for enhanced mass loss that smoothly grows from the single star wind mass loss rate to the Roche lobe overflow mass loss rate as the radius of the star approaches its Roche lobe radius. This gives a variable mass loss rate along eccentric orbits that is higher at orbital phases closer to the periastron, even if the star does not fill its Roche lobe. This effect works in the same way as discussed

above, but no filling of the Roche lobe is needed, so that (during the AGB phase) this effect is permanently competing against tidal circularisation.

Boffin & Jorissen (1988) carried out calculations of the variation of orbital parameters considering instantaneous mass transfer and only linear momentum conservation. Angular momentum conservation was not taken into account in this exploratory study. An extension including angular momentum conservation was made by Liu et al. (2000), but they make use of the orbital average of the distance between the components and orbital angular velocity to carry out their calculations, which in the case of a variable mass loss along the orbit does not give the correct results.

In Sect. 2 we revise the variation of orbital parameters due to stellar mass loss and mass transfer by taking into account the conservation laws of linear and angular momentum with respect to the centre of mass of the actual binary system. We do not make use of the orbital averages a priori, but give the variations as a function of the orbital phase, allowing different rates of mass loss and mass transfer along the orbit. In Sect. 3 we calculate the rate of change of the eccentricity according to different assumptions of mass loss and accretion. In Sect. 4 we evaluate the competition between the tidal circularisation and the eccentricity pumping due to our proposed mass loss, and show that the latter can prove effective in counteracting the former for systems such as Sirius and barium stars in which their AGB component did not fill its Roche lobe. A summary is presented in Sect. 5.

## 2. Variational analysis of orbital parameters due to wind mass transfer or mass loss

The dynamics of a binary orbit are well described by the two masses, $M_1$ and $M_2$, its energy, $E_{\text{orb}}$, and its angular momentum, $J_{\text{orb}}$ (e.g., Goldstein 1980). The fractional variation of the semimajor axis (also called the separation), $a$, and of the eccentricity, $e$, are expressed as

$$\frac{\delta a}{a} = \frac{\delta M}{M} + \frac{\delta m}{m} - \frac{\delta E_{\text{orb}}}{E_{\text{orb}}} \tag{1}$$

and

$$\frac{\delta(1 - e^2)}{(1 - e^2)} = 2\frac{\delta J_{\text{orb}}}{J_{\text{orb}}} + \frac{\delta E_{\text{orb}}}{E_{\text{orb}}} - 2\frac{\delta M}{M} - 3\frac{\delta m}{m}, \tag{2}$$

where we use the notation for the reduced mass problem, such that the total mass $M \equiv M_1 + M_2$ and the reduced mass $m \equiv \frac{M_1 M_2}{M_1 + M_2}$. For a detailed derivation of these expressions and those that follow in this section see Appendix A.

### 2.1. Angular momentum and energy

In a system where $r$ is the instantaneous distance between the stars and $\omega$ is the instantaneous angular velocity of the components with respect to a co-moving inertial frame with its origin in the centre of mass (from here on the CM frame), the fractional variations of orbital angular momentum and energy are given by

$$\frac{\delta J_{\text{orb}}}{J_{\text{orb}}} = \frac{\delta m}{m} + 2\frac{\delta r}{r} + \frac{\delta \omega}{\omega}$$
$$= \frac{\delta m}{m} + \frac{\delta r}{r} + \frac{\delta v_\theta}{v_\theta} \tag{3}$$

and

$$\frac{\delta E_{\text{orb}}}{E_{\text{orb}}} = \frac{\delta m}{m} + \frac{2a}{r}\frac{\delta M}{M} - \frac{2a}{r}\frac{\delta r}{r} - \frac{a}{GM}[2v_r\delta v_r + 2v_\theta\delta v_\theta] \tag{4}$$

respectively. We denote the velocity of one star relative to its companion by $\boldsymbol{v} = \boldsymbol{v_1} - \boldsymbol{v_2}$, where $\boldsymbol{v_i}$ is the velocity of star $i$ with respect to the CM. $\boldsymbol{v}$ also corresponds to the orbital velocity in the reduced mass problem. We also use the subscripts $r$ and $\theta$ to indicate the radial and transverse velocity components respectively.

We consider a system in which both stars may lose mass in isotropic winds, part of which may be accreted by the companion such that during a time interval $\delta t$ an amount of mass $\delta M_{1,\text{W}}$ is lost by star 1 and an amount $\delta M_{2,\text{ACC}}$ is accreted by star 2. In this way an amount of mass $\delta M_{1,\text{LOST}} = \delta M_{1,\text{W}} - \delta M_{2,\text{ACC}}$ is effectively lost by star 2 from the system. To determine how the orbital velocity components vary we assume that star 2 receives an impulse when it accretes an amount of mass $\delta M_{2,\text{ACC}}$ coming from the wind of star 1, which at the moment it is accreted has a velocity $\boldsymbol{w_{12}}$ in the CM frame. The corresponding expressions for mass lost from star 2 are obtained by interchanging the indices 1 and 2. This yields the variations

$$\delta v_r = \left[w_{r,12} - v_{r,2}\right]\frac{\delta M_{2,\text{ACC}}}{M_2} + (1 \Leftrightarrow 2), \tag{5}$$

and

$$\delta v_\theta = \left[w_{\theta,21} - r_2\omega\right]\frac{\delta M_{2,\text{ACC}}}{M_2} + (1 \Leftrightarrow 2) \tag{6}$$

where $r_i$ corresponds to the distances of star $i$ to the CM. The notation $+(1 \Leftrightarrow 2)$ used here and below means: add terms to the left again with indices 1 and 2 interchanged. For quantities defined with an index in the left-hand side of the equation it is implicit that the corresponding expression for the other star is obtained by exchanging the indices in the right-hand side. By means of Eqs. (3)−(6) we can now write the orbital angular momentum and energy variations as

$$\frac{\delta J_{\text{orb}}}{J_{\text{orb}}} = -\frac{\delta M_{1,\text{LOST}}}{M_1}\left(\frac{M_2}{M}\right)$$
$$+ \frac{\delta M_{2,\text{ACC}}}{M_2}\left(1 - \frac{M_2}{M_1} + \frac{w_{\theta\text{rel},2}}{r\omega}\right) + (1 \Leftrightarrow 2) \tag{7}$$

and

$$\frac{\delta E_{\text{orb}}}{E_{\text{orb}}} = -\frac{\delta M_{1,\text{LOST}}}{M_1}\left[1 + \left(\frac{2a}{r} - 1\right)\frac{M_1}{M}\right]$$
$$+ \frac{\delta M_{2,\text{ACC}}}{M_2}\left[1 - \frac{M_2}{M_1} - \frac{2a}{GM}\boldsymbol{v} \cdot \boldsymbol{w_{\text{rel},2}}\right] + (1 \Leftrightarrow 2). \tag{8}$$

In these equations $\boldsymbol{w_{\text{rel},2}} \equiv (\boldsymbol{w_{12}} - \boldsymbol{v_2})$ is the relative velocity of the wind with respect to star 2 when accreted. We have also used the fact that there must be no displacements $\delta r_i$, which implies that $\delta r/r = 0$ (see Appendix A for details).

### 2.2. Behaviour of the wind

To apply these expressions in calculations of orbital evolution, the detailed behaviour of the wind as it travels through the system must be followed from its point of origin until it is accreted or escapes the binary potential well. In general this requires either ballistic calculations (e.g., Brookshaw & Tavani 1993) or full-scale hydrodynamical calculations (e.g., Theuns et al. 1996; Nagae et al. 2004). For the purpose of this paper we assume the simple model described below.

The velocity of the wind from star $j$ when it is accreted by star $i$ has a radial component, $w_{r,ji}$, that we will assume to be the

velocity of the wind emanating isotropically from star $j$ as if it were a single star, $w_j$. For the transverse component, $w_{\theta,ji}$, we assume that the specific angular momentum of the wind with respect to the CM is conserved and we express it as $h_{W,j} \equiv \chi_j r_j^2 \omega$. Note that the wind carries both the orbital and spin angular momentum of the mass-losing star. With the above definition $\chi_j = 1$ represents a point mass, given that such an idealised object can only carry orbital angular momentum and no intrinsic spin. Once the wind is accreted by the companion star $i$ a fraction $\mu_i$ of $h_{W,j}$ is transferred to the spin angular momentum of the accretor and the rest is transferred to the orbit. Thus $w_{\theta,ji} = \xi_j \frac{M_i^2}{M^2} \frac{h_{orb}}{r_i}$, where $h_{orb}$ is the orbital specific angular momentum given by $h_{orb}^2 = r^4 \omega^2 = GMa(1 - e^2)$ and $\xi_1 \equiv \chi_1(1 - \mu_2)$, which yields

$$(w_{\theta,12} - r_2\omega) = r\omega \left( \frac{\xi_1 M_2^2 - M_1^2}{M_1 M} \right), \tag{9}$$

and similar for $w_{\theta,21} - r_1\omega$.

## 3. Rate of eccentricity change

More useful than arbitrary variations of the physical parameters are their rates of change in time, thus from this point on we will transform $\delta \to \mathrm{d}/\mathrm{d}t$. The distance and orbital velocity components are

$$\frac{a}{r} = \frac{1 + e\cos\theta}{1 - e^2},$$

$$v_r = \sqrt{\frac{G(M_1 + M_2)}{a(1 - e^2)}} e \sin\theta \quad \text{and} \tag{10}$$

$$v_t = \sqrt{\frac{G(M_1 + M_2)}{a(1 - e^2)}}(1 + e\cos\theta),$$

where $\theta$ is the orbital phase angle measured from the periastron. It is clear from its dependence on the orbital phase-angle that $\dot{e}$ is not constant along the orbit. This is true for constant mass loss and accretion rates, but especially if mass loss and accretion rates also depend on the orbital phase angle. Employing the results we have derived so far we calculate using Eq. (2)

$$\dot{e} = \frac{\dot{M}_{1,\mathrm{LOST}}(\theta)}{M}\{e + \cos\theta\}$$
$$+ \frac{\dot{M}_{2,\mathrm{ACC}}(\theta)}{M_2}\left\{ \frac{M_1}{M}\left[ \left( \frac{\xi_1 M_2^2}{M_1^2} - 1 \right)(2\cos\theta + e + e\cos^2\theta) \right. \right.$$
$$\left. \left. - e\sin^2\theta \right] + w_1 \sqrt{\frac{a(1 - e^2)}{GM}} \sin\theta \right\} + (1 \Leftrightarrow 2). \tag{11}$$

We note that the first term only depends on the assumption of isotropic mass loss and it is the same as given by Soker (2000) (see also Eggleton 2006). It shows that the eccentricity can increase if the mass loss rate is higher near periastron than near apastron. The second term also depends on the additional assumptions about the wind behaviour (see Sect. 2.2). These are complicated expressions that must be followed along the orbit if they are to have a useful meaning. The orbital period is given by $P = 2\pi \sqrt{\frac{a^3}{G(M_1+M_2)}}$ and by defining the orbital average of a parameter $A$ as $\langle A \rangle \equiv \frac{1}{P}\int_0^P A\,\mathrm{d}t = \frac{1}{P}\int_0^{2\pi} A\frac{\mathrm{d}t}{\mathrm{d}\theta}\mathrm{d}\theta$ we compute the net rate of change of $a$ and $e$ in one orbital period. When an orbital average is applied to Eq. (11) we obtain an expression that

depends on $\langle \dot{M}_{i,\mathrm{LOST}} \rangle$, $\langle \dot{M}_{i,\mathrm{LOST}} \cos\theta \rangle$, $\langle \dot{M}_{i,\mathrm{ACC}} \rangle$, $\langle \dot{M}_{i,\mathrm{ACC}} \cos\theta \rangle$, $\langle \dot{M}_{i,\mathrm{ACC}} \sin\theta \rangle$, $\langle \dot{M}_{i,\mathrm{ACC}} \cos^2\theta \rangle$ and $\langle \dot{M}_{i,\mathrm{ACC}} \sin^2\theta \rangle$ for $i = 1, 2$. These averages can be calculated only after $\dot{M}_{i,\mathrm{LOST}}(\theta)$ and $\dot{M}_{i,\mathrm{ACC}}(\theta)$ are known.

### 3.1. Constant wind and constant mass accretion

Usually the simplest case is assumed which corresponds to when $\dot{M}_{i,\mathrm{ACC}} = \langle \dot{M}_{i,\mathrm{ACC}}(\theta) \rangle$ and $\dot{M}_{i,\mathrm{LOST}} = \langle \dot{M}_{i,\mathrm{LOST}}(\theta) \rangle$ are constant along the orbit (e.g., Hurley et al. 2002). This yields

$$\frac{\langle \dot{e} \rangle}{e} = -\frac{\dot{M}_{2,\mathrm{ACC}}}{M_2}\left( \frac{(1 - \sqrt{1 - e^2})}{e^2} \frac{(1 - e^2)\xi_1 M_2^2}{M_1 M} \right) + (1 \Leftrightarrow 2). \tag{12}$$

Clearly with the assumptions about the wind made here the eccentricity can only decrease, therefore if this effect is comparable to that of tidal friction it will only help to circularise the orbit on a faster timescale, otherwise it can be neglected (Hurley et al. 2002[1]).

### 3.2. Accretion from a fast isotropic wind

We model the mass accretion with the Bondi & Hoyle (1944) mechanism, in which

$$\dot{M}_{2,\mathrm{ACC}}(\theta) = \alpha \frac{(GM_2)^2 \dot{M}_{1,\mathrm{W}}}{r_A^2 w_{\mathrm{rel},2}^3 w_1}, \tag{13}$$

where $\dot{M}_{1,\mathrm{W}}$ is the wind mass loss rate from star 1, $r_A$ the distance to the source of the wind at the moment it was emitted and $\alpha$ is a numerical factor that parameterises the efficiency of the accretion mechanism. In the case of a steady isotropic wind much faster than the orbital motion the transverse component of the wind velocity can be neglected, therefore one can safely assume that $w_{\mathrm{rel},2} = w_1$ and $r_A = r$. Then the accretion rate $\dot{M}_{2,\mathrm{ACC}}(\theta) = \dot{M}_{2,0\ \mathrm{ACC}}(1 + e\cos\theta)^2$, where $\dot{M}_{2,0\ \mathrm{ACC}} = \frac{\langle \dot{M}_{2,\mathrm{ACC}}(\theta) \rangle}{\langle(1 + e\cos\theta)^2\rangle}$. The mass from star 1 that is lost from the system is given by $\dot{M}_{1,\mathrm{LOST}} = \dot{M}_{1,\mathrm{W}} - \dot{M}_{2,\mathrm{ACC}}$. With this assumption the averaged rate of change of $e$ is

$$\frac{\langle \dot{e} \rangle}{e} = \frac{\dot{M}_{2,0\ \mathrm{ACC}}}{M_2}$$
$$\times \frac{(1 - e^2)^{3/2}}{2M_1(M_1 + M_2)}\left( 3\xi_j M_2^2 - 2M_1(M_2 + 2M_1) \right) + (1 \Leftrightarrow 2). \tag{14}$$

In contrast to Eq. (12), where $e$ always decreases with time, Eq. (14) shows that the eccentricity will increase if $M_2/M_1 > \left( 1 + \sqrt{1 + 12\xi_1} \right)/3\xi_1$ (e.g., $M_1 \lesssim 0.65M_2$ for the case of point masses, where $\xi_1 = 1$).

### 3.3. Accretion from the slow wind of an AGB star

The case of an AGB star with an accreting companion is somewhat different from the two cases we have already reviewed. The velocity of the wind from an AGB star is of the order of the stellar escape velocity, which is also of the order of the orbital velocity, if the size of the AGB star is a significant fraction of its Roche lobe. This implies that $w_1 \sim \sqrt{\frac{GM}{a(1-e^2)}}$, so the transverse

---

[1] Hurley et al. (2002) have a different expression for $\dot{e}/e$ due to different assumptions made in their calculations, however, their expression and ours are of the same order of magnitude.

velocity of the wind cannot be neglected as in the fast-wind case. Thus, making use of Eqs. (9) and (10) we write

$$w_{\text{rel},2}{}^2(\theta) = \left( \frac{GM}{a(1-e^2)} \right)$$

$$\times \left[ \left( \frac{w_1}{\sqrt{\frac{GM}{a(1-e^2)}}} - \frac{M_1 e \sin \theta}{M} \right)^2 + \left( \frac{[\xi_1 M_2{}^2 - M_1{}^2](1 + e \cos \theta)}{M_1 M} \right)^2 \right] \quad (15)$$

and by means of Eq. (13) we express the accretion rate as

$$\dot{M}_{2,\text{ACC}}(\theta) = \frac{\dot{M}_{2,0\ \text{ACC}}(1 + e \cos \theta)^2}{\left[ \left( \frac{w_1}{\sqrt{\frac{GM}{a(1-e^2)}}} - \frac{M_1 e \sin \theta}{M} \right)^2 + \left( \frac{[\xi_1 M_2{}^2 - M_1{}^2](1 + e \cos \theta)}{M_1 M} \right)^2 \right]^{3/2}},$$

$$(16)$$

where $\dot{M}_{2,0\ \text{ACC}} = \left( \frac{GM}{a(1-e^2)} \right)^{3/2} \langle \dot{M}_{2,\text{ACC}}(\theta) \rangle \langle \frac{w_{\text{rel},2}{}^3(\theta)}{(1+e\cos\theta)^2} \rangle$ in this case. The orbital average can be only calculated numerically, but we find that when $w_1 \gtrsim 3 \sqrt{\frac{GM}{a(1-e^2)}}$ the result of the integration is well approximated by the fast-wind assumption. The fact that the orbital phase can change significantly between the moment the wind was emitted and when it is accreted also introduces a phase angle shift in the relation between $\dot{M}_{2,\text{ACC}}$ and $\dot{M}_{1,\text{W}}$. However, we performed numerical calculations of $\langle \dot{e} \rangle / e$ by applying different phase angle shifts in Eq. (13) and the results do not differ by more than 15% from the zero phase-angle case.

### 3.4. Mass loss from an AGB star

A non-AGB star has a steep density gradient in its photospheric layers, i.e., it has a well defined radius. When the star is smaller than its Roche lobe any mass loss is in the form of a wind which may be enhanced by the presence of the companion (e.g., Tout & Eggleton 1988). If such a star becomes larger than its Roche lobe then the mass loss rate is abruptly enhanced by orders of magnitude, governed by the Roche lobe overflow mechanism. Thus there is an almost discontinuous transition from one regime to the other and they can be treated as separate cases. AGB stars, on the other hand, have a shallow surface density gradient (e.g., Bowen 1988; Pastetter & Ritter 1989) and therefore the transition between the wind and the Roche lobe overflow mass loss regimes is smooth. Karovska et al. (2005) made observations in X-rays of the symbiotic binary system Mira which show the AGB star is surrounded by material in the shape of a lobe as predicted by the Roche model. This suggests that the star is undergoing a transitional form of mass loss that can be described as wind Roche-lobe overflow. This provides support to the idea that the extended and weakly-bound atmosphere of an AGB star can be highly influenced by the tidal force exerted by the companion. Frankowski & Tylenda (2001) computed the enhancement of the wind mass loss rate of giant stars in binary systems through the effect of the Roche potential on the local surface temperature and gravity. They find that the mass loss enhancement depends on $(R_\star/R_{\text{L}})^3$, where $R_\star$ and $R_{\text{L}}$ are radius of the AGB star and its Roche-lobe radius, respectively. However, the overall effect is modest, less than a factor of 2, unless $R_\star$ is very close to $R_{\text{L}}$. Their model does not account for the wind Roche-lobe overflow transition expected for AGB stars and suggested by the observations of Mira. Tout & Eggleton (1988) propose that the mass loss rate of cool giants is enhanced by the presence of a companion, driven by the tidal friction torque. Thus, in their heuristic

model the mass loss enhancement depends on the sixth power of the $R_\star/R_{\text{L}}$ ratio. Building on this idea, we propose the following AGB star mass loss model, which provides a smooth transition between the single-star wind mass loss rate, $\dot{M}_{\star,\text{w}}$, and the Roche-lobe overflow mass loss rate, $\dot{M}_{\text{RLOF}}$:

$$\dot{M}_\star = \dot{M}_{\star,\text{W}} \left[ 1 + \left( \frac{\dot{M}_{\text{RLOF}}}{\dot{M}_{\star,\text{W}}} - 1 \right) \left( \frac{R_\star}{R_{\text{L}}} \right)^6 \right]. \quad (17)$$

For eccentric orbits the Roche geometry does not apply so we utilise an *instantaneous* Roche-lobe that depends on the actual distance between the stars, $r$, as

$$R_{\text{L}}(\theta) = \frac{a(1-e^2)}{(1 + e \cos \theta)} f(q_\star), \quad (18)$$

where $q_\star$ is the mass ratio of the AGB star to its companion and $f(q) = \frac{0.49 q^{2/3}}{0.6 q^{2/3} + \ln(1 + q^{1/3})}$, following the approximation of Eggleton (1983). With this prescription the mass loss rate along the orbit is not constant, but enhanced when the system is at orbital phases close to the periastron. Thus, if the AGB star does not fill its Roche lobe in the periastron and there is no mass transfer ($\dot{M}_{i,0\ \text{ACC}} = 0$), the net contribution in one orbital period to the eccentricity variation rate is

$$\frac{\langle \dot{e} \rangle}{e} = \frac{\dot{M}_{\text{RLOF}} - \dot{M}_{\star,\text{W}}}{M} \left( \frac{R_\star}{af(q_\star)} \right)^6 \frac{3(8 + 12e^2 + e^4)}{8(1-e^2)^{9/2}}. \quad (19)$$

Equation (19) will always contribute to enhance the eccentricity, given that $\dot{M}_{\text{RLOF}}$ is larger than $\dot{M}_{\text{AGB,W}}$. The effect of mass transfer to the companion will in many cases act against the eccentricity enhancement, but its contribution to Eq. (19) cannot be expressed analytically and it has to be calculated numerically (see Sects. 3.2 and 3.3). However, it becomes significant only when a considerable amount of mass lost from the AGB star is transferred.

## 4. Comparison of timescales

In this section we calculate and compare the timescales on which the effects of circularisation and eccentricity enhancement will take place, $\tau_{\text{circ}}$ and $\tau_e$ respectively. Hurley et al. (2002) give the following expression for the tidal evolution of $e$ due to convective damping by combining the results of Zahn (1977, see also Zahn & Bouchet 1989) and Hut (1981):

$$\frac{1}{\tau_{\text{circ}}} \equiv -\frac{\dot{e}}{e} = \frac{18}{7} \frac{f_{\text{conv}}}{\tau_{\text{conv}}} \frac{M_{\text{env}}}{M_\star} \frac{(1 + q_\star)}{q_\star^2 (1-e^2)^{13/2}} \left( \frac{R_\star}{a} \right)^8$$

$$\times \left[ f_3(e^2) - \frac{11}{18}(1-e^2)^{3/2} f_4(e^2) \frac{\Omega_{\star,\text{s}}}{n} \right], \quad (20)$$

where $M_{\text{env}}$ is the envelope mass of the AGB star and $\tau_{\text{conv}}$ is the convective turnover timescale. A good approximation to the depth of the convective zone in an AGB star is its radius, thus by employing Eq. (31) from Hurley et al. (2002) we obtain $\tau_{\text{conv}} = 0.2351(M_{\text{env}}R_\star^2/L_\star)^{1/3}$yr, with $L_\star$ the luminosity of the star and the parameters expressed in solar units. $\Omega_{\star,\text{s}}/n$ is the ratio of spin angular rotation rate of the AGB star, $\Omega_{\star,\text{s}}$, to the average orbital angular velocity, $n$. The functions $f_x(e^2)$ are those derived by Hut (1981) and the numerical factor $f_{\text{conv}} = f' \min \left( 1, (P_{\text{tid}}/2\tau_{\text{conv}})^2 \right)$ is from Rasio et al. (1996), where $P_{\text{tid}}^{-1} = |n - \Omega_{\star,\text{s}}|/2\pi$. Verbunt & Phinney (1995) found from an analysis of observed red-giant binaries that $f' \approx 1$, however, this value may be different for

the case of AGB stars. It is important to note that this calculation of $\tau_{\text{circ}}$ gives a stronger circularising effect for orbits with finite eccentricity values than the usually employed prescription by Zahn (1977) which assumes an almost circular orbit (e.g., Rasio et al. 1996; Soker 2000).

We estimate the Roche-lobe overflow mass loss rate $\dot{M}_{\text{RLOF}}$ following the prescription of Ritter (1988, see also Meyer & Meyer-Hofmeister 1983; Pastetter & Ritter 1989), where

$$\dot{M}_{\text{RLOF}} = \frac{2\pi}{\sqrt{e}} \left( \frac{k_B}{m_H \mu_\star} T_\star \right)^{3/2} \frac{R_\star^{\ 3}}{GM_\star} \rho_{\star,\text{ph}} F(q_\star^{-1}), \tag{21}$$

with $F(x) = 1.23 + 0.5 \log x$. The photospheric density of the AGB star is given by (Kippenhahn & Weigert 1990; Soker 2006)

$$\rho_{\star,\text{ph}} = \frac{2}{3} \frac{m_H \mu_\star}{k_B} \frac{GM_\star}{R_\star^2 \kappa_\star\ T_\star}, \tag{22}$$

where $\kappa_\star$ is the opacity of the envelope of the AGB star and $\mu_\star$ and $T_\star$ are the mean molecular weight and effective temperature of the stellar surface, respectively. $m_H$ is the mass of the hydrogen atom and and $k_B$ is the Boltzmann constant. A typical $1.5-2.5\ M_\odot$ AGB star has a surface temperature of about 3300 K, a radius of about 300 $R_\odot$ and a luminosity of about $10\,000\ L_\odot$. Most of the surface material in such a star is weakly ionised due to the low surface temperature, so we assume a typical surface molecular weight of 1.3 (see e.g., Soker 2006). According to the envelope opacity calculations of Marigo (2002), the corresponding opacity at this temperature is approximately $\kappa_\star = 2.5 \times 10^{-4}$ cm$^2$ g$^{-1}$ for densities of the order of $10^{-13}-10^{-11}$ g cm$^{-3}$, which is the expected range of AGB surface densities. Employing this value of $\kappa_\star$ and the luminosity, radius, mass and mean molecular weight mentioned above, the prescription of Eq. (21) yields $\dot{M}_{\text{RLOF}} \sim 10^{-3}\ M_\odot$ yr$^{-1}$. This is about $10\,000-30\,000$ times larger than the single-star wind mass loss rate of our typical star at the beginning of the AGB lifetime, calculated with the prescription of Vassiliadis & Wood (1993). By the end of the AGB phase, at the onset of the superwind phase, $\dot{M}_{\text{RLOF}}$ is still $50-200$ times larger than the wind mass loss rate.

### 4.1. Eccentricity of the Sirius system

Sirius A, a main sequence star of 2.1 $M_\odot$, and Sirius B, a white dwarf of 1.05 $M_\odot$ (Gatewood & Gatewood 1978), form a binary system with period $P = 50.1$ yr and eccentricity $e = 0.59$ (van den Bos 1960). Given the semi-major axis of the orbit, $a = 20$ AU, and the eccentricity of this system, the distance between its components at periastron is about 1700 $R_\odot$. By the time the primary star (initially a star of about $5.5-6\ M_\odot$) was in the AGB phase its radius was so large ($R \approx 750\ R_\odot$) that it could have filled its Roche lobe during periastron passages. Whether or not the Roche lobe was filled, a strong tidal interaction must have occurred due to the proximity of the system components. We have tracked the evolution of binary systems that evolve into a main sequence star with the mass of Sirius A and a white dwarf with the mass of Sirius B, which from here on we will call Sirius-like systems. To compute the binary evolution models we employed a version of the rapid synthetic code of binary evolution of Izzard et al. (2006), which makes use of modifications described in Bonačić Marinović et al. (2007). The code
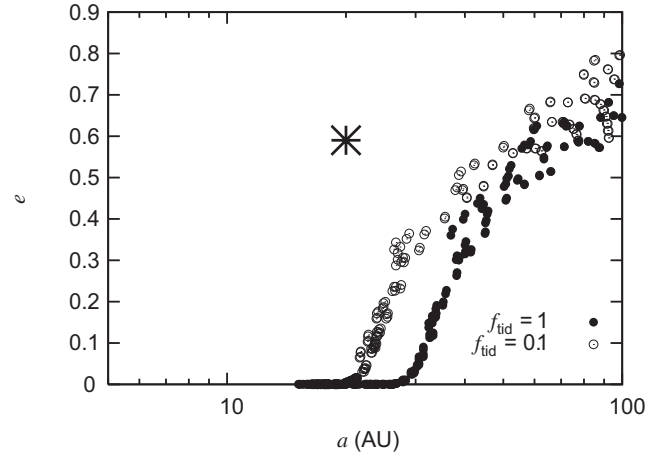


**Fig. 1.** Computed eccentricity of Sirius-like binary models without any eccentricity-enhancing mechanism as function of their separation, assuming the standard binary interaction. The filled circles indicate the orbital parameters of Sirius-like systems computed by assuming a tidal dissipation factor $f' = 1$. The open circles are similar, but assuming that the tidal dissipation is ten times weaker. The star indicates the observed orbital parameters of the Sirius system, which has a notably higher eccentricity than what standard models predict for its separation, even with substantially reduced tidal friction.

employs Eq. (20) to model the effect of circularisation. The set of initial conditions for the models consists of the following:

- a primary with initial mass of 5.7 $M_\odot$, which ends its life as a white dwarf similar to Sirius B, independently of the choice of mass loss;
- 2 initial secondary masses (2.00 and 2.05 $M_\odot$) which yield a star similar to Sirius A;
- 25 initial separations, $a_i$, logarithmically separated between 10 AU and 500 AU;
- 25 initial eccentricities, separated linearly between 0.5 and 0.99;
- solar metallicity, $Z = 0.02$.

In the standard scenario of tidal dissipation with constant mass loss along the orbit the eccentricity will always decrease. Figure 1 shows the distribution of the synthetic Sirius-like systems in the $a-e$ plane compared to the observed position of the Sirius system in this plane. The solid circles indicate the orbital properties of Sirius-like systems when assuming $f' = 1$, which show that the standard scenario of tidal interaction in binary evolution predicts complete circularisation for systems separated up to about 30 AU. The closest system with an eccentricity of 0.59 has a separation of about 55 AU. When the strength of tidal dissipation is reduced to $f' = 0.1$ (open circles), the predicted orbital parameters are still far from reproducing the observed Sirius system. A separation of at least about 40 AU is required to obtain the observed eccentricity of 0.59. To reproduce the eccentricity and separation of Sirius within this scenario a tidal dissipation factor $f' < 10^{-3}$ is needed, which is too strong a reduction to be acceptable. This demonstrates that the standard scenario of binary evolution cannot explain the observed eccentricity of the Sirius system, because it predicts that the system should be circularised.

However, this is not the case if the tidally enhanced mass loss we propose in Eq. (17) is considered. Due to its variable mass loss along the orbit an eccentricity-enhancing effect counteracts the tidal circularisation. We compare $\tau_e$ and $\tau_{\text{circ}}$ to see which effect is dominant. We estimate their values at the moment of

evolution when the tidal dissipation effects are strongest, which is the bottleneck for ending up with an eccentric orbit. This occurs when the AGB star reaches its maximum radius, 700 $R_\odot$, at which point it has a luminosity of 38 000 $L_\odot$ and a core and envelope mass of 1.0 $M_\odot$ and 3.5 $M_\odot$ respectively. For the calculation of the Roche-lobe overflow mass loss rate we assume $\kappa_\star = 10^{-4}$, which approximates the values calculated by Marigo (2002) for the envelope opacity of high-metallicity stars with a temperature of about 3000 K. This gives $\dot{M}_{RLOF} = 1.944 \times 10^{-3}\ M_\odot\ yr^{-1}$ according to Eq. (21), while the wind mass loss rate at this point is $\dot{M}_{\star,W} = 5.168 \times 10^{-5}\ M_\odot\ yr^{-1}$. While mass loss from a system tends to increase its separation, the tidal interaction tends to (pseudo-)synchronise the rotation of the AGB star with the orbit and thereby shrink the orbit due to transfer of orbital angular momentum. This orbital shrinking effect is especially strong in the beginning of the AGB phase, when the star expands rapidly and rotates slowly. However, once the AGB star rotation approaches a (pseudo-)synchronised rate with the orbit, the widening of the orbit due to mass loss dominates over the effect of tidal shrinking. Assuming this last regime, Fig. 2 shows how the $a-e$ plane is divided into a region where the eccentricity decreases (upper-left area) and a region where the eccentricity is enhanced (lower-right area). Thus, if we adopt a modest reduction of the tidal dissipation strength ($f' = 0.5$), any system with a separation larger than about 14 AU will eventually cross to the eccentricity-enhancing region, avoiding a circular orbit by the end of the AGB phase. In particular, the orbit of a system with orbital parameters similar to Sirius will remain eccentric. The thin dotted and dashed lines in Fig. 2 show that the location of the dividing line between decreasing and increasing eccentricity is sensitive to the tidal strength factor $f'$. This is because the ratio of timescales $\tau_e/\tau_{circ}$ only varies as $(R_\star/a)^2$, i.e., a much weaker dependence than either of the individual timescales. There is a similar sensitivity to the adopted average opacity $\kappa_\star$ through $\dot{M}_{RLOF}$, which is also not certain, given that Eq. (21) is only approximate. Given these uncertainties, the results are not definitive. However, we have shown that by adopting reasonable values for the uncertain parameters the orbit of Sirius can be kept significantly eccentric. Finally we note that the results are insensitive to the amount of mass accreted by the companion, as long as this is less than about 10−15% of the mass lost by the AGB star.

So far we have shown how our eccentricity-enhancing mechanism works by employing values of single-star models for the AGB primary at a given moment of evolution. However, the overall effect on the orbit of a given binary depends on how the relevant parameters change as a function of time as the binary evolves from zero age to its current state. We have therefore implemented the orbital evolution formulae derived in Sect. 3 into the synthetic binary evolution code of Izzard et al. (2006), including our enhanced mass loss prescription. Full details of this implementation are given in Bonačić Marinović & Pols (2007). We calculate models for the same set of initial conditions as described above. The choice of the amount of mass that the companion accretes does not affect our results significantly, unless it is larger than about 15% of the total mass lost by the primary. We assume that 5% of the enhanced mass loss ($\dot{M}_\star - \dot{M}_{\star,W}$) is accreted by the companion, which increases the final mass of the secondary to that of Sirius A. Figure 3 shows a comparison of the synthetic Sirius-like systems resulting from these models to the observed orbital properties of Sirius. The filled circles show the eccentricity and separation predicted by models that assume the standard tidal dissipation, $f' = 1$. Compared to the case when only tidal dissipation is considered (Fig. 1), the resulting binaries are significantly more eccentric in the
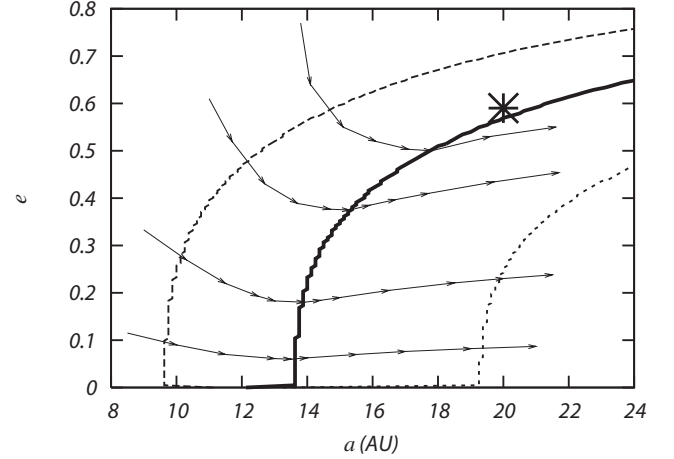


**Fig. 2.** Behaviour of eccentricity of a binary system with a 4.5 $M_\odot$ AGB primary (initially a 5.5 $M_\odot$ star) and a 2.1 $M_\odot$ MS secondary as the system widens due to mass loss. The thick solid line indicates $\tau_e = \tau_{circ}$ when $f'$ is assumed to be 0.5 and 5% of the mass lost via the enhanced mass loss mechanism is accreted by the companion. The arrows indicate instantaneous directions in the diagram that a binary system will follow as it evolves. The star represents the current position in the $a-e$ plane of the Sirius system. The thin dashed and dotted lines also indicate $\tau_e = \tau_{circ}$, but considering $f' = 0.25$ and $f' = 1$, respectively.
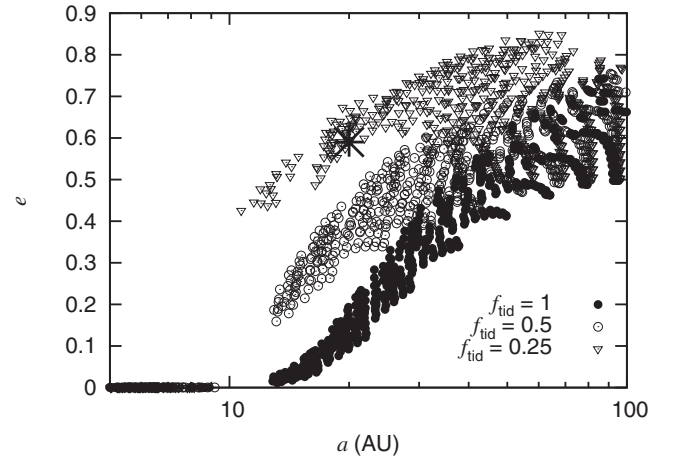


**Fig. 3.** Computed eccentricity of Sirius-like binary models that take into account our proposed eccentricity enhancing mechanism plotted as function of their separation. The filled circles indicate the orbital parameters of Sirius-like systems computed by assuming a tidal dissipation factor $f' = 1$. The open circles and triangles indicate the results for similar calculations, but assuming that the tidal dissipation factor $f'$ is 0.5 and 0.25, respectively. The star indicates the observed orbital parameters of the Sirius system, which are well reproduced if $f' = 0.25$ is assumed.

separation range 15-40 AU, and the effect is comparable to reducing the tidal strength to $f' = 0.1$ in Fig. 1. To reproduce the orbital properties of Sirius, the tidal dissipation has to be weakened by only a factor of 4 (triangles in Fig. 3), which is still within a range of reasonable values, as opposed to a reduction by more than a factor 1000 needed when only tidal circularisation is included.

### 4.2. Eccentricities of the barium stars

Barium stars show over-abundances of s-process elements, most prominently of barium, and are found in binary systems with
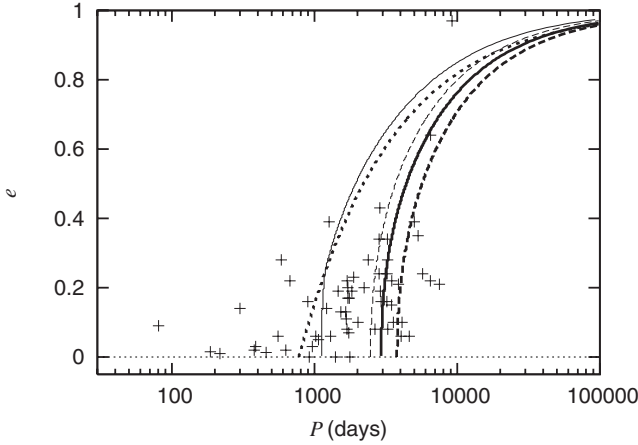
**Fig. 4.** Distribution in the $P-e$ plane of barium star and the limits for circularisation set by different models. The crosses indicate the observational data of barium stars form Jorissen et al. (1998). The thick lines delimit the regions where eccentric and circularised orbits are expected and are calculated for a system as described in the text, by assuming a tidal dissipation factor $f' = 1$. The thin lines show the same limits as the thick lines, but this time calculated by assuming $f' = 0.1$. Solid lines indicate the circularisation limit when the eccentricity-pumping mechanism we propose is considered. The dashed lines show the circularisation limit in the standard scenario. The dotted line indicates the limit for which Roche lobe overflow occurs at the periastron and the horizontal thin dotted line indicates $e = 0$.

white dwarf companions. This constitutes evidence for mass accretion from their companions when the latter were asymptotic giant branch (AGB) stars, given that s-process elements are synthesised in the AGB phase of evolution. Barium star binary systems are observed to have periods between 80 and 10 000 days and most of the systems with periods longer than about 600 days are significantly eccentric (see Fig. 4). These systems pose a problem to the standard binary evolution scenario which predicts that orbits with periods shorter than about 3500−4000 days should have been circularised due to the tidal dissipation that must have taken place when the primary was an AGB star (e.g., Pols et al. 2003). The eccentricity enhancement resulting from our proposed AGB mass loss provides a mechanism that can effectively compete with tidal circularisation. We calculate the relevant timescales for a binary system with a 1.5 $M_\odot$ AGB primary and a 1.1 $M_\odot$ secondary, with metallicity $Z = 0.008$. We assume that 10% of the mass lost by the AGB star is accreted by the companion, so that the latter accretes enough material to enhance its s-process element abundances significantly and become a barium star. The calculations are made at the AGB stage of evolution where the tidal dissipation is strongest (the circularisation bottleneck), where the radius of the AGB star is 280 $R_\odot$, its luminosity is 7500 $L_\odot$ and its core and envelope masses are 0.64 $M_\odot$ and 0.6 $M_\odot$ respectively. Applying these values to Eq. (21) we obtain that $\dot{M}_{RLOF} = 1.75 \times 10^{-3}$ $M_\odot$ yr$^{-1}$ according to Eq. (21), while the wind mass loss rate at this point is $\dot{M}_{\star,W} = 1.02 \times 10^{-5}$ $M_\odot$ yr$^{-1}$.

Our results are shown in Fig. 4 and are compared to the observed data from Jorissen et al. (1998) in the $P-e$ plane. The thick dashed line separates the region where the orbits will be circularised (to the left of the line) from the region where eccentric orbits are possible (to the right of the line) in the standard binary scenario, where only the tidal circularisation is acting. This limit is calculated by assuming $\tau_{circ}^{-1} = M/\dot{M}$ and a tidal dissipation factor $f' = 1$, and reasonably well reproduces the limit

resulting from binary population synthesis calculations (e.g., Pols et al. 2003). The majority of the systems cannot be explained in this picture. The thick solid line indicates the same limit, but with the eccentricity-pumping mechanism included, i.e., when $|\tau_e^{-1} - \tau_{circ}^{-1}| = M/\dot{M}$. The evolution of binary systems in the $P-e$ plane is similar to that in the $a-e$ plane (shown in Fig. 2), thus the eccentricities of the systems to the right of the thick line can be explained. This means that with the default tidal strength the eccentricity-enhancement mechanism cannot compete effectively with the tidal circularisation, except for a very limited period range around 3000 days. However, the tidal dissipation factor $f'$ is not very certain for AGB stars, given that it has been measured to be approximately unity mostly using observations of red giants (Verbunt & Phinney 1995). Hence it is reasonable to calculate the circularisation limits for lower values of $f'$, as our calculations for the Sirius system suggest. Figure 4 shows in thin lines the same limits that we have already described above, but assuming $f' = 0.1$. In this case the eccentricity of almost all systems that do not fill their Roche-lobes can be explained. Karakas et al. (2000) found that with a similar choice of $f'$ they could reproduce the eccentricities of all observed barium stars, including those with periods less than 1000 days. In their simulations they included a tidally enhanced AGB mass loss rate as well, but without any eccentricity-enhancing mechanism to compete against tidal circularisation. However, the results they report are difficult to understand in the light of our findings, especially because they excluded all systems in which the AGB star filled its Roche lobe. The systems to the left of the thick dotted line in Fig. 4 fill their Roche lobes during the AGB and in most cases enter a common envelope (CE) phase. The evolution of the orbit during this phase is not a well understood problem and is also beyond the scope of this study. However, it seems more likely that an already eccentric system which enters a CE phase may remain eccentric than that a circular system becomes eccentric during the CE phase. Thus a mechanism that at least allows orbits to remain eccentric until the point when Roche-lobe overflow occurs may be necessary to explain the eccentric systems that are to the left of the Roche-lobe limit. As shown in Fig. 4, assuming weak tidal friction with $f' = 0.1$ makes it possible that systems with an AGB primary fill their Roche lobe with a significant eccentricity.

It is important to note that the reduction of the tidal strength needed to explain the eccentricities of most observed barium-star systems that did not fill their Roche lobe ($f' = 0.1$) is calculated for one specific system, assumed to be representative. In order to test whether the eccentricity-enhancing mechanism explains the properties of the barium stars, the full evolutionary history has to be followed (as in the case of Sirius) for a variety of system parameters in a binary population synthesis study. Furthermore, not only the orbital parameters have to be reproduced, but also their abundance distributions. Such an analysis is beyond the scope of this work and we will present it in a subsequent paper. Preliminary results of population synthesis of barium stars indicate that $f' = 0.25$ is needed for reproducing the eccentricities of most observed systems that have not filled their Roche lobes, which is consistent with the reduction of tidal dissipation strength needed to reproduce the orbit of the Sirius system.

## 5. Conclusions

We have revised the description of the evolution of orbital parameters due to mass loss and mass transfer in a binary system where the primary is an AGB star. We also propose a tidally

enhanced mass loss rate for AGB stars in binary systems, which allows a smooth transition between wind mass loss and mass loss due to Roche lobe overflow. With our revised prescription for the evolution of the orbital eccentricity and the fact that our proposed mass loss is not constant along an eccentric orbit, we find an eccentricity-enhancing mechanism that counteracts the circularising effect of tidal dissipation. We have shown that the standard scenario of binary interaction cannot explain the observed orbital parameters of the eccentric binary system Sirius, unless the strength of tidal dissipation in AGB stars is at least 3 orders of magnitude smaller than in normal red giants. On the other hand, our models with the eccentricity-enhancing mechanism can reproduce the orbital properties of the Sirius system with a reasonable choice of the tidal dissipation parameter ($f' = 0.25$). Our eccentricity-enhancing mechanism also allows binary systems containing barium stars to remain eccentric with periods as short as about 1000 days under reasonable parameter assumptions, while under the same assumptions in the standard scenario of tidal circularisation only systems with periods longer than about 2500 days are expected to show a significant eccentricity. We also show that we can explain the eccentricities of almost all barium-star systems that do not fill their Roche lobes if the uncertain convective tidal dissipation strength in AGB stars is reduced by a factor of 10 compared to what is measured for red giant stars. Moreover, this assumption allows Roche-lobe overflow to occur in significantly eccentric systems, which may be the key to explain shorter-period barium-star systems that are still eccentric.

Whether our eccentricity-enhancing mechanism is a viable solution to the problem of explaining short-period eccentric binaries with (former) AGB stars, in particular barium stars, needs to be tested with a binary population synthesis model. Results of such a test will be given in a separate paper (Bonačić Marinović & Pols 2007). Preliminary barium-star population synthesis calculations indicate that when the full evolutionary history of a binary population is taken into account, a reduction of the tidal dissipation strength of only $f' = 0.25$ is needed to reproduce the observed systems. This is consistent with our findings about the values of $f'$ needed to reproduce the Sirius system.

## Appendix A: Derivation of variation of orbital parameters

The orbit of a binary star system can be described by the eccentricity $e$ and the semi-major axis $a$. The change in these orbital parameters can be related to changes in the masses $M_{1,2}$ of the two stars, either due to mass loss or mass accretion, through the conservation laws for the total orbital energy $E_{\text{orb}}$ and the orbital angular momentum $J_{\text{orb}}$, given by

$$E_{\text{orb}} = -\frac{GMm}{2a},\tag{A.1}$$

and

$$J_{\text{orb}}^2 = m^2 r^4 \omega^2 = GMm^2 a(1 - e^2).\tag{A.2}$$

Here $\omega$ is the instantaneous angular velocity, $r$ is the instantaneous separation among the system components, $M = M_1 + M_2$ is the total mass and $m = M_1 M_2 / M$ is the reduced mass of the
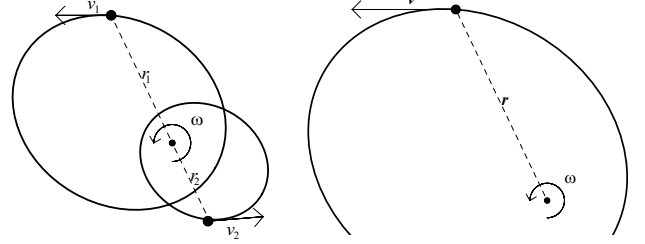


**Fig. A.1.** The geometric relation between the positions and velocities of both components in a binary system (*left*) and the equivalent reduced mass problem (*right*).

system. The variations of the orbital parameters $a$ and $e$ are then given by

$$\frac{\delta a}{a} = \frac{\delta M}{M} + \frac{\delta m}{m} - \frac{\delta E_{\text{orb}}}{E_{\text{orb}}}\tag{A.3}$$

and

$$\frac{\delta(1 - e^2)}{1 - e^2} = 2\frac{\delta J_{\text{orb}}}{J_{\text{orb}}} + \frac{\delta E_{\text{orb}}}{E_{\text{orb}}} - 2\frac{\delta M}{M} - 3\frac{\delta m}{m}.\tag{A.4}$$

In the following we will derive expressions for $\delta E_{\text{orb}}$ and $\delta J_{\text{orb}}$.

### A.1. Variation of the orbital energy

The total orbital energy is the sum of the kinetic energy and the gravitational energy,

$$E_{\text{orb}} = \frac{1}{2}mv^2 - \frac{GM_1 M_2}{r},\tag{A.5}$$

where $r = |\boldsymbol{r}_1 - \boldsymbol{r}_2|$ is the instantaneous distance between the two stars and $\boldsymbol{v} = \boldsymbol{v}_1 - \boldsymbol{v}_2$ is their relative velocity (see Fig. A.1). The variation of (A.5) is given by

$$\delta E_{\text{orb}} = \frac{1}{2}mv^2\left(\frac{\delta m}{m} + \frac{\delta(v^2)}{v^2}\right) - \frac{GMm}{r}\left(\frac{\delta M}{M} + \frac{\delta m}{m} - \frac{\delta r}{r}\right).\tag{A.6}$$

The velocity $\boldsymbol{v}$ has components $v_r$ and $v_\theta = r\omega$ in polar coordinates, so that the variation of $\delta(v^2)$ can be written as

$$\delta(v^2) = 2v_r \delta v_r + 2r\omega\left(r\delta\omega + \omega\delta r\right).\tag{A.7}$$

For later use, we will need to know the variation in terms of the variations for the individual components,

$$\delta(v^2) = 2v_r \delta v_{r,1} + 2r\omega(r_1\delta\omega + \omega\delta r_1) + (1 \Leftrightarrow 2).\tag{A.8}$$

The notation $+(1 \Leftrightarrow 2)$ means: add terms to the left again with indexes 1 and 2 interchanged. Note that this is an addition despite $\boldsymbol{v}$ being defined as the difference $\boldsymbol{v}_1 - \boldsymbol{v}_2$. The reason is that contrary to a Cartesian basis the direction of basis vectors in polar coordinates is not fixed but depends on the angular coordinate $\theta$.

We will consider two effects that change the mass of each star: Bondi-Hoyle accretion (Bondi & Hoyle 1944) and isotropic mass loss. The latter does not affect the velocity of the star relative to the centre of mass, but the former does. Let $\delta M_1 = \delta M_{1,\text{ACC}}$ denote the mass accreted by star 1 and let $\boldsymbol{w}_{21}$ be the velocity of the wind of star 2 at the moment it is accreted by star 1 and $\boldsymbol{w}_{12}$ vice versa. Then conservation of momentum gives

$$M_1\delta\boldsymbol{v}_1 = (\boldsymbol{w}_{21} - \boldsymbol{v}_1)\,\delta M_{1,\text{ACC}}\tag{A.9}$$

and similar for star 2. Inserting this in (A.8) gives the relation

$$\delta(v^2) = 2\boldsymbol{v} \cdot (\boldsymbol{w}_{21} - \boldsymbol{v}_1)\frac{\delta M_{1,\text{ACC}}}{M_1} + (1 \Leftrightarrow 2).\tag{A.10}$$

It now remains to express $\delta M$ and $\delta m$ in terms of the variation of the individual masses $\delta M_1$ and $\delta M_2$. For the purpose of bookkeeping we split the mass lost from star 1 (and similarly for star 2) into two parts: the amount $\delta M_{1,\text{LOST}}$ that is lost from the system and the amount $\delta M_{2,\text{ACC}}$ that is eventually accreted by star 2. Then

$$\delta M_1 = -\delta M_{1,\text{LOST}} - \delta M_{2,\text{ACC}} + \delta M_{1,\text{ACC}} \tag{A.11}$$

and

$$\delta M_2 = -\delta M_{2,\text{LOST}} - \delta M_{1,\text{ACC}} + \delta M_{2,\text{ACC}}. \tag{A.12}$$

The variation of the total mass $\delta M$ is just $\delta M_1 + \delta M_2$ while the variation of the reduced mass is

$$\frac{\delta m}{m} = -\frac{\delta M_{1,\text{LOST}}}{M_1} \frac{M_2}{M_1 + M_2} + \frac{\delta M_{1,\text{ACC}}}{M_1} \left(1 - \frac{M_1}{M_2}\right) + (1 \Leftrightarrow 2). \tag{A.13}$$

If the transfer of momentum due to the wind is instantaneous the distance $r$ between the two stars is not changed, hence $\delta r = 0$. Inserting (A.8), (A.11), (A.12) and (A.13) into (A.6) then gives

$$\frac{\delta E_{\text{orb}}}{E_{\text{orb}}} = \frac{\delta M_{1,\text{ACC}}}{M_1} \left[1 - \frac{M_1}{M_2} - \frac{2a}{G(M_1 + M_2)} \boldsymbol{v} \cdot (\boldsymbol{w}_{21} - \boldsymbol{v}_1)\right] - \frac{\delta M_{1,\text{LOST}}}{M_1} \left[1 + \left(\frac{2a}{r} - 1\right)\frac{M_1}{M_1 + M_2}\right] + (1 \Leftrightarrow 2) \tag{A.14}$$

which is the same as (8).

### A.2. Variation of the orbital angular momentum

The variation of the orbital angular momentum (A.2) is

$$\frac{\delta J_{\text{orb}}}{J_{\text{orb}}} = \frac{\delta m}{m} + \frac{\delta r}{r} + \frac{\delta v_\theta}{v_\theta}, \tag{A.15}$$

where as before $v_\theta = r\omega$. Using (A.9), (A.13) and the fact that $r$ does not depend on the variation of the two masses immediately gives

$$\frac{\delta J_{\text{orb}}}{J_{\text{orb}}} = \frac{\delta M_{1,\text{ACC}}}{M_1} \left(1 - \frac{M_1}{M_2} + \frac{w_{\theta,21} - r_1\omega}{r_1\omega}\right) - \frac{\delta M_{1,\text{LOST}}}{M_1} \frac{M_2}{M_1 + M_2} + (1 \Leftrightarrow 2) \tag{A.16}$$

which is the same as (7).

### A.3. The Variation of the semi-major axis

The variation of the eccentricity that results from the above considerations is given in (11) in the text. For completeness we here give the corresponding expression for the variation in $a$. Inserting (A.14) and (A.13) in (A.3) we obtain

$$\frac{\delta a}{a} = \frac{\delta M_{1,\text{ACC}}}{M_1} \frac{2a}{G(M_1 + M_2)} \boldsymbol{v} \cdot (\boldsymbol{w}_{21} - \boldsymbol{v}_1) + \frac{\delta M_{1,\text{LOST}}}{M_1} \frac{M_1}{M_1 + M_2} \left(\frac{2a}{r} - 1\right) + (1 \Leftrightarrow 2). \tag{A.17}$$

## References

Boffin, H. M. J., & Jorissen, A. 1988, A&A, 205, 155
Bonačić Marinović, A. A., & Pols, O. R. 2007, in preparation
Bonačić Marinović, A., Izzard, R. G., Lugaro, M., & Pols, O. R. 2007, A&A, 469, 1013
Bondi, H., & Hoyle, F. 1944, MNRAS, 104, 273
Bowen, G. H. 1988, ApJ, 329, 299
Brookshaw, L., & Tavani, M. 1993, ApJ, 410, 719
Eggleton, P. P. 1983, ApJ, 268, 368
Eggleton, P. 2006, Evolutionary Processes in Binary and Multiple Stars (Cambridge, UK: Cambridge University Press), ISBN 0521855578
Frankowski, A., & Tylenda, R. 2001, A&A, 367, 513
Gatewood, G. D., & Gatewood, C. V. 1978, ApJ, 225, 191
Goldstein, H. 1980, Classical mechanics, 2nd edn., Addison-Wesley Series in Physics
Hurley, J. R., Tout, C. A., & Pols, O. R. 2002, MNRAS, 329, 897
Hut, P. 1981, A&A, 99, 126
Izzard, R. G., Dray, L. M., Karakas, A. I., Lugaro, M., & Tout, C. A. 2006, A&A, 460, 565
Jorissen, A., Van Eck, S., Mayor, M., & Udry, S. 1998, A&A, 332, 877
Karakas, A. I., Tout, C. A., & Lattanzio, J. C. 2000, MNRAS, 316, 689
Karovska, M., Schlegel, E., Hack, W., Raymond, J. C., & Wood, B. E. 2005, ApJ, 623, L137
Kippenhahn, R., & Weigert, A. 1990 Stellar Structure and Evolution, XVI (Berlin, Heidelberg, New York: Springer-Verlag), also Astronomy and Astrophysics Library
Liu, J. H., Zhang, B., Liang, Y. C., & Peng, Q. H. 2000, A&A, 363, 660
Marigo, P. 2002, A&A, 387, 507
Meyer, F., & Meyer-Hofmeister, E. 1983, A&A, 121, 29
Nagae, T., Oka, K., Matsuda, T., et al. 2004, A&A, 419, 335
Pastetter, L., & Ritter, H. 1989, A&A, 214, 186
Pols, O. R., Karakas, A. I., Lattanzio, J. C., & Tout, C. A. 2003, in ASP Conf. Ser. 303, ed. R. L. M. Corradi, J. Mikolajewska, & T. J. Mahoney (Astronomical Society of the Pacific Conference Series), 290
Rasio, F. A., Tout, C. A., Lubow, S. H., & Livio, M. 1996, ApJ, 470, 1187
Ritter, H. 1988, A&A, 202, 93
Soker, N. 2000, A&A, 357, 557
Soker, N. 2006, New Astron., 11, 396
Theuns, T., Boffin, H. M. J., & Jorissen, A. 1996, MNRAS, 280, 1264
Tout, C. A., & Eggleton, P. P. 1988, MNRAS, 231, 823
van den Bos, W. H. 1960, J. Observateurs, 43, 145
Van Winckel, H., Waelkens, C., & Waters, L. B. F. M. 1995, A&A, 293, L25
Vassiliadis, E., & Wood, P. R. 1993, ApJ, 413, 641
Verbunt, F., & Phinney, E. S. 1995, A&A, 296, 709
Waelkens, C., Van Winckel, H., Waters, L. B. F. M., & Bakker, E. J. 1996, A&A, 314, L17
Waters, L. B. F. M., Cami, J., de Jong, T., et al. 1998, Nature, 391, 868
Zahn, J.-P. 1977, A&A, 57, 383
Zahn, J.-P., & Bouchet, L. 1989, A&A, 223, 112